國立交通大學

電子工程學系電子研究所碩士班

碩 士 論 文

利用銅整合製程製作仿酢醬草結構之感測振膜麥克風

A Micromachined Microphone with Oxalis-like Electroplated Cu Sensing Diaphragm for Sound Source Localization

研 究 生：劉 濬 誠

指導教授：鄭 裕 庭 教授

中 華 民 國 九 十 六 年 十 月

利用銅整合製程製作仿酢醬草結構之感測振膜麥克風

A Micromachined Microphone with Oxalis-like Electroplated Cu Sensing Diaphragm for Sound Source Localization

研 究 生：劉濬誠　　Student：Chun-Cheng Liu

指導教授：鄭裕庭　　Advisor：Yu-Ting Cheng

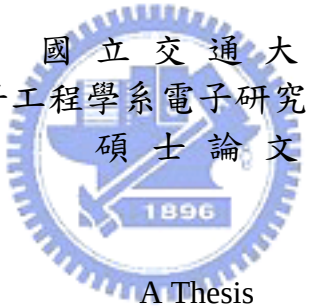

國 立 交 通 大 學
電子工程學系電子研究所碩士班

碩 士 論 文

A Thesis

Submitted to Department of Electronics Engineering & Institute of Electronics
College of Electrical and Computer Engineering
National Chiao-Tung University
in Partial Fulfillment of the Requirements
for the Degree of Master
in
Electronics Engineering
October 2007

Hsinchu, Taiwan, Republic of China

中華民國九十六年十月

利用銅整合製程製作仿酢醬草結構之感測振膜麥克風

學生：劉濬誠　　指導教授：鄭裕庭教授

國立交通大學電子工程學系暨電子研究所碩士班

摘　　要

本文提出一個有仿酢醬草結構感測振膜的銅電鍍仿生式麥克風，這個振膜設計採用中文學名為奧米亞棕蠅的聽覺感測機制 [5,6] 但是藉由感測振膜的去耦而有更好的靈敏度。在麥克風的設計上，總共有六片感測葉片透過彎曲彈簧互相連結並且接合於中央平衡支撐結構，此結構由各六個內外支樞連結到一個環上。在 60dB 聲音位準下，反相模式變形讓此結構有最大淨位移量 0.02091 μm，極化圖顯示此結構有 25°±20%的空間分辨率。因為可以使用傳統電鍍製程製作麥克風，所以低製作成本和小尺寸讓此結構在助聽器應用上變得極好。

A Micromachined Microphone with Oxalis-like Electroplated Cu Sensing Diaphragm for Sound Source Localization

Student : Chun-Cheng Liu Advisor : Yu-Ting Cheng

Department of Electronics Engineering & Institute of Electronics

National Chiao Tung University

Abstract

This paper presents a Cu electroplated biomimetic microphone with oxalis-like sensing diaphragms. This diaphragm design follows the acoustic sensing mechanism of parasitoid fly (Orima Ochracea) [5,6] but has larger sensitivity by decoupling the sensing diaphragm. In the microphone design, there are total six sensing leaves connected each other by serpentine springs and supported by a central gimbal structure which has six inner and six outer pivots connected to a circle ring. Under 60dB SPL, the device can have maximum 0.02091μm net displacement in a reversed-mode deformation. The polar pattern shows the device has 25°±20% opening angles. Because the microphone can be fabricated using conventional electroplating process, low manufacturing cost and small form factor will make the device fascinating for hearing aid applications.

誌　謝

歷經漫長的求學生涯，終於要在這暫時畫下句點，這也算是人生一大歷練，心中難免激動不已。

首先當然得感謝家人的支持，一路走來始終沒讓我為學費煩惱過，只是為了期盼我能夠專心讀書、學以致用，媽媽經常打電話來噓寒問暖，姊姊在我心情不好時都能夠給予我安慰及鼓勵，爸爸雖對成績要求甚高，但也就因為如此才能造就我現在的學業，只能有說不完的謝謝。

此外還要感謝我的指導老師鄭裕庭教授，在我面臨困難及疑問時能夠指點迷津讓我能夠有勇氣面對挑戰，非常感謝老師的指導，尤其在畢業的前夕讓你操心了，謝謝你對我的教誨。再來就是要感謝一路有幫助到我的學長學姊，尤其要感謝機械所徐文祥實驗室的學長們，讓我順利完成實驗，最後量測階段幫我大忙的 CIC 工讀生及儀器設備，我才能順利畢業。

最後當然要感謝實驗室的每一位麻吉，包括時常被我問問題的博班學長子元及建章、新進來的印度研究生 Singh，大一屆的 chando、小 B、昱文和詩穎，同輩幫我機台許多的文駿和睿婉，以及後期幫我的永昌、韋廷、茄子和家瑋，以及新生碩一要接我後路的學弟們，此外還有帶我們吃好吃的助理小筑囉，希望畢業後大家不要太想我，祝大家能夠延續實驗室的傳統精神，好好努力拼畢業吧!!

Contents

中文摘要 ..... **i**

Abstract ..... **ii**

誌謝 ..... **iii**

Contents ..... **iv**

Figure Captions ..... **v**

Table Captions ..... **vii**

Chapter 1 Introduction **1**

Chapter 2 Comparison of the Structure by Silicon and Copper **4**

2.1The Structure of the Biomimetic Microphone 4

2.2 ANSYS Simulation and Polar Pattern 5

Chapter 3 Microphone Fabrication **8**

Chapter 4 Result and Measurement **10**

4.1 Result of SEM Graph 10

4.2 Measurement 11

4.3 Discussion 15

Chapter 5 Conclusion and Future Work **20**

5.1 Conclusion 20

5.2 Future Work 20

References **21**

Figure Captions

Chapter 2

Fig. 2-1 The optimum design of the oxalis-like diaphragm [7] 5

Fig. 2-2 The illustrations of (a) the displacement under 60dB SPL (b) in-phase resonant mode (c) y-axis reversed-phase resonant mode (d) x-axis reversed-phase resonant mode 6

Fig. 2-3 The polar pattern of the net displacement of silicon and copper by applying a pressure load 60dB SPL (0.02Pa) on the right half side (reference displacement of copper : 1.975 μm ; of silicon : 1.048 μm) 7

Chapter 3

Fig. 3-1 Process sequence for the biomimetic diaphragm of the microphone 9

Chapter 4

Fig. 4-1 (a) The entire view of the microphone is photographed by SEM 10

Fig. 4-1 (b) The enlarge view photographs focus on the serpentine spring and central gimbals region respectively 11

Fig. 4-2 A experiment setup for measuring the microphone 12

Fig. 4-3 The resonant frequency of the diaphragm measured by MMA and simulation 12.13

Fig. 4-4 The plot of the displacement of the diaphragm to the amplitude of the sound source between reality and simulation 14

Fig. 4-5 The polar pattern of net displacement of the diaphragm in 60dB SPL,

300Hz (reference displacement in simulation : 1.975 μ m ; in reality : 0.00704 μ m) 14

Fig. 4-6 (a) The surface roughness of the central gimbal region obtained by WYKO analysis system 15

Fig. 4-6 (b) The surface roughness of the one diaphragm region obtained by WYKO analysis system 16

Fig. 4-7 The correction structure by ANSYS simulation 17

Fig. 4-8 The ANSYS simulation of the correction deformation of the diaphragm 17.18

Table Captions

Chapter 2

Table 2-1 Comparison of the microphone properties between silicon and copper 6

Chapter 4

Table 4-1 Comparison of the microphone properties between reality and simulation 19

Chapter 1 Introduction

The microphone is a mechtronic component transforming acoustic energy into electrical one. It developed rapidly in recent years with a variety of applications including conferences, entertainments, audiovisuals, medical service and so on. Using MEMS technology to fabricate a microphone can greatly reduce its manufacturing cost and form factor. Meanwhile, sound-localization has been one of the research topics in the development of modern microphone since the functions can reduce the nonessential background noise and provide more accurate sound to user. In 2002, Nobukata Ono, etc, one of these teams studying such a microphone design, proposed the MEMS typed biomimetic mechanism with center-supported diaphragm for a very small pressure gradient caused by the sound field [1-4]. This idea came from the parasitoid fly Ormia Ochracea's special acoustic organ [5,6]. The structure can provide 360 degrees of freedom in the directional response and create mechanical coupling to the in-phase and reversed-phase vibration modes used for determining the originated direction of sound source.

In 2006, Ching et al. proposed oxalis-like sensing diaphragm design to enhance the sensitivity of the aforementioned biomimetic microphone in terms of the enlargement of displacement by decoupling the six equally divided diaphragms [7]. The microphone uses a condenser typed sensing mechanism which provides many advantages like flat frequency responses in wide

bandwidth, low noise level, good stability, high sensitivity, and low driving power [8]. However, we want to propose other material like metal which can make the same device also integrated with IC chips for miniaturization and SOC (System on Chip). According to the article which mentions the post-CMOS process [9], Tinghui Xin et al. took the advantage of LIGA-like process and pulse electroplating technique to fabricate microprobe using metals including Cu. Ni and so on. In consideration of feasibility and characteristics among them, copper is an adaptable in this process because the experiment equipment for electroplating is installed easily and material used is low cost.

On the other hand, copper has better conductivity than silicon and can ensure better performance of condenser microphone. The copper process can be controlled under 100℃ and this low temperature is convenient for integrating IC process. As far as the sensitivity of microphone is concerned, the equation [10] is given by follow:

$$S = \frac{V_b}{d_0} \cdot \frac{1}{\frac{\pi^2 E h^3}{3a^4(1-\nu^2)} + \frac{\pi^2 \sigma h}{a^2}} \cdot \frac{C_m}{C_m + C_s}$$

where V_b is bias voltage, d_o is air gap length, a is the half length of the diaphragm's edge, h is the thickness of the diaphragm, C_m is capacitance of the microphone, C_s is the stray capacitance, σ is the tensile stress of the diaphragm, E is the Young's Modulus, and vis the Poisson's ratio. Among these parameters,

Young's Modulus and Poisson's ratio are important values standing for material property. Although the sensitivity of copper is lower than one of silicon, we can reduce the thickness of diaphragm to redeem the decrease and increase the sensitivity. Finally, we decide to use copper as the material of the microphone's diaphragm in process.

Chapter 2 Comparison of the Structure by Silicon and Copper

2.1 The Structure of the Biomimetic Microphone

The microphone is based on my senior Wen Hao Ching's optimum design that is the central-supported structure with six leave connected each other by six serpentine springs, six inner and six outer supporting beams combined with one ring. The radius of the diaphragm is 2500μm, each inner supporting beam is 100μm long and 10μm wide, each outer support beam is 30μm long and 10μm wide and a 20μm-wide ring. Each serpentine spring is 20μm wide and total 300μm long in Fig.2-1. But we decrease the thickness of the diaphragm to 4μm in order to fit my copper process.

This size of the design is optimized by a number of simulations and some physical theorems including the sensitivity, the number of the diaphragm, the shape of the serpentine spring, and the ratio of inner supporting beam length to outer supporting beam length.

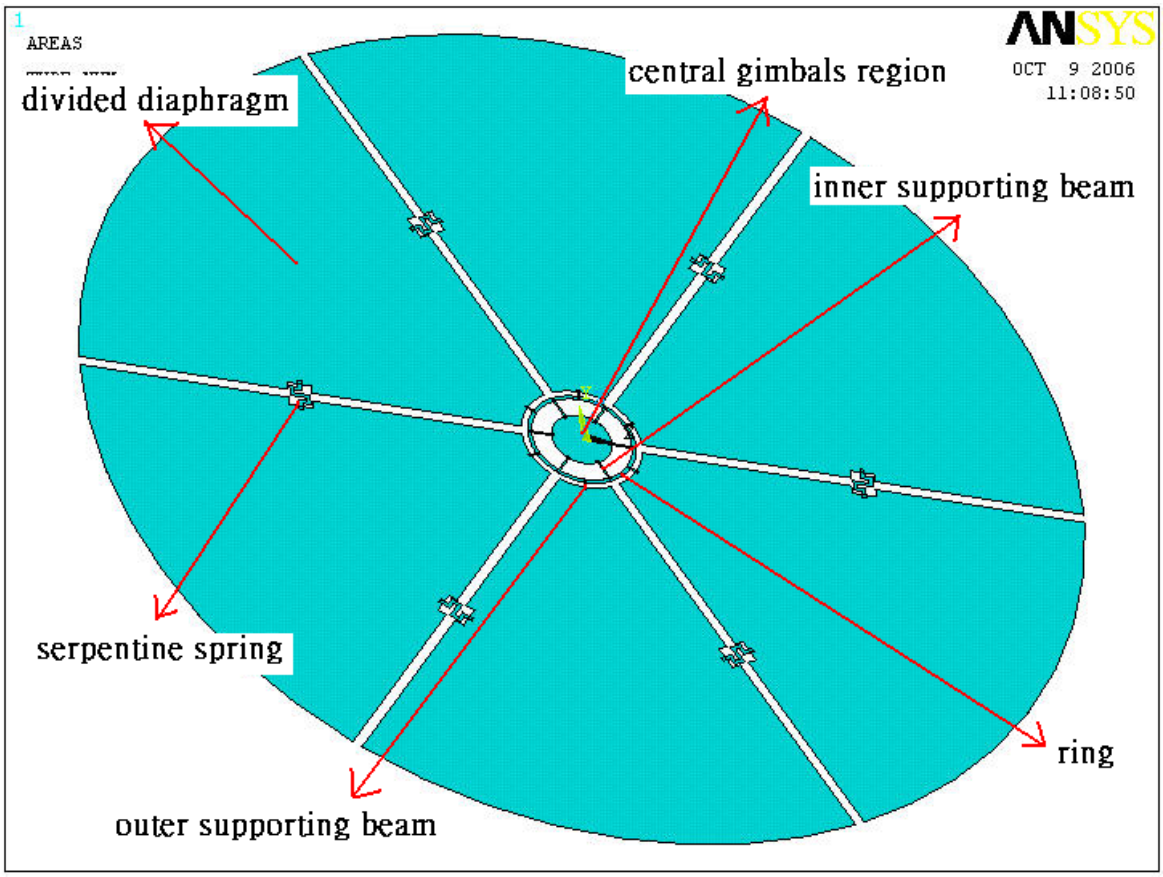

Fig. 2-1 The optimum design of the oxalis-like diaphragm [7]

2.2 ANSYS Simulation and Polar Pattern

Now we use ANSYS [11] software to simulate the same structure performance again by changing the material property. Table 2-1 shows the comparisons of the microphone between silicon and copper including the net displacement of the diaphragm along z-axis by applying a pressure load 60dB SPL which is the most comfortable volume for people on the right half side, in-phase, y-axis reversed-phase and x-axis reversed-phase resonant mode frequency. All simulated illustrations shown in Fig. 2-2. The maximum net displacement of copper is 2.04μm, almost twice of silicon (1.0768μm). Three

resonant mode frequencies of copper are less than one of silicon because the structure is softer by decrease of the thickness.

Comparison between Si and Cu	60dB Maximum net displacement	in-phase resonant mode	y-axis reversed-phase resonant mode	x-axis reversed-phase resonant mode
Silicon(5μm)	1.0768μm	256.998Hz	261.751Hz	261.945Hz
Copper(4μm)	2.04μm	109.02Hz	110.13Hz	110.21Hz

Table 2-1 Comparisons of the microphone properties between silicon and copper

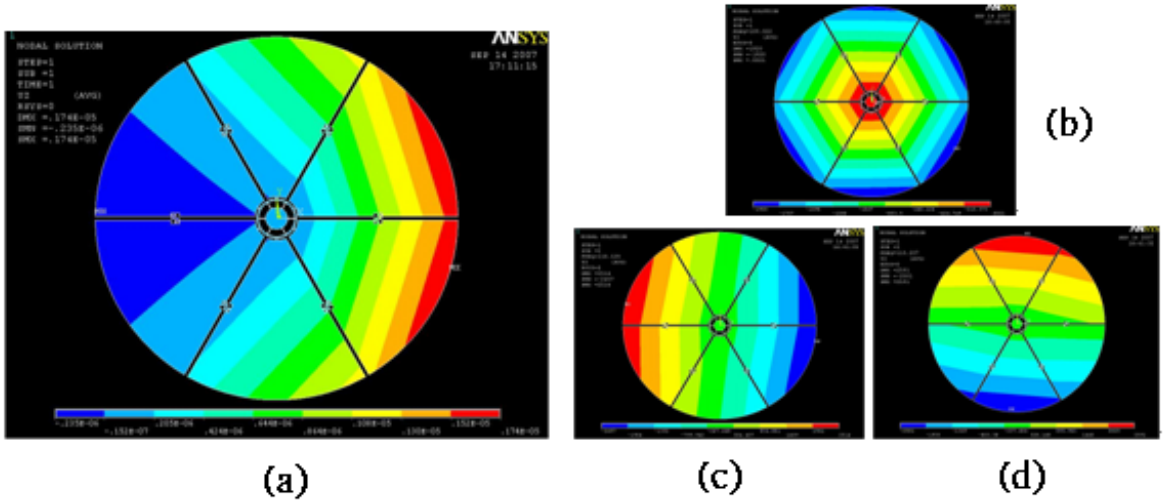

Fig. 2-2 The illustrations of (a) the displacement under 60dB SPL (b) in-phase resonant mode (c) y-axis reversed-phase resonant mode (d) x-axis reversed-phase resonant mode.

The polar pattern shown in Fig. 2-3 presents that the opening angle of copper is 10 degrees which is identical to one of silicon and the opposite displacement of copper is better than one of silicon. This advantage can make the estimation of direction more easily.

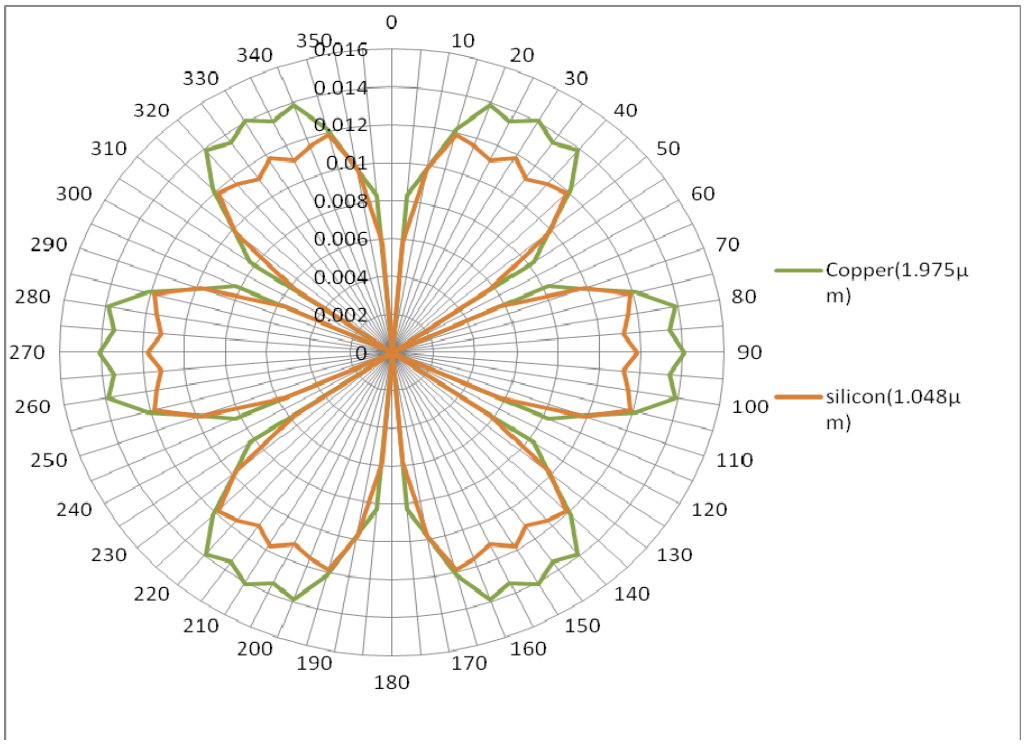

Fig. 2-3 The polar pattern of the net displacement of silicon and copper by applying a pressure load 60dB SPL (0.02Pa) on the right half side (reference displacement of copper: 1.975μm; of silicon: 1.048μm)

Chapter 3 Microphone Fabrication

The fabrication process sequence of microphone is depicted in Fig. 3-1.

(a) We use the furnace system to deposit about 0.7μm thermal wet oxidation at 1050℃ on a 4" (100)-orient silicon wafer and sputter Ti/Cu (300Å/900Å) adhesion/seed layers on the isolation layer.

(b) The region of the diaphragm as bottom electrode is defined by a patterned 2μm-thick AZ4620 photo-resist and using copper electroplating to fill the region.

(c) A 8μm-thick AZ4620 photo-resist is spin-coated and patterned as the sacrificial layer to define the region of the center-support pillar.

(d) Electroplating copper in the region about 6μm to flatten the structure and sputtering a 900Å copper seed layer for realizing the upper electrode.

(e) Another 4μm-thick AZ4620 photo-resist is spin-coated and patterned to define the region of the diaphragm as upper electrode. The region is filled by electroplating copper.

(f) We use acetone and positive photo-resist stripper to remove the sacrificial layer completely, and utilize CR-7T and BOE to etch the seed/adhesion layer. Finally, we use hotplate (35℃) to release the structure dunked in IPA

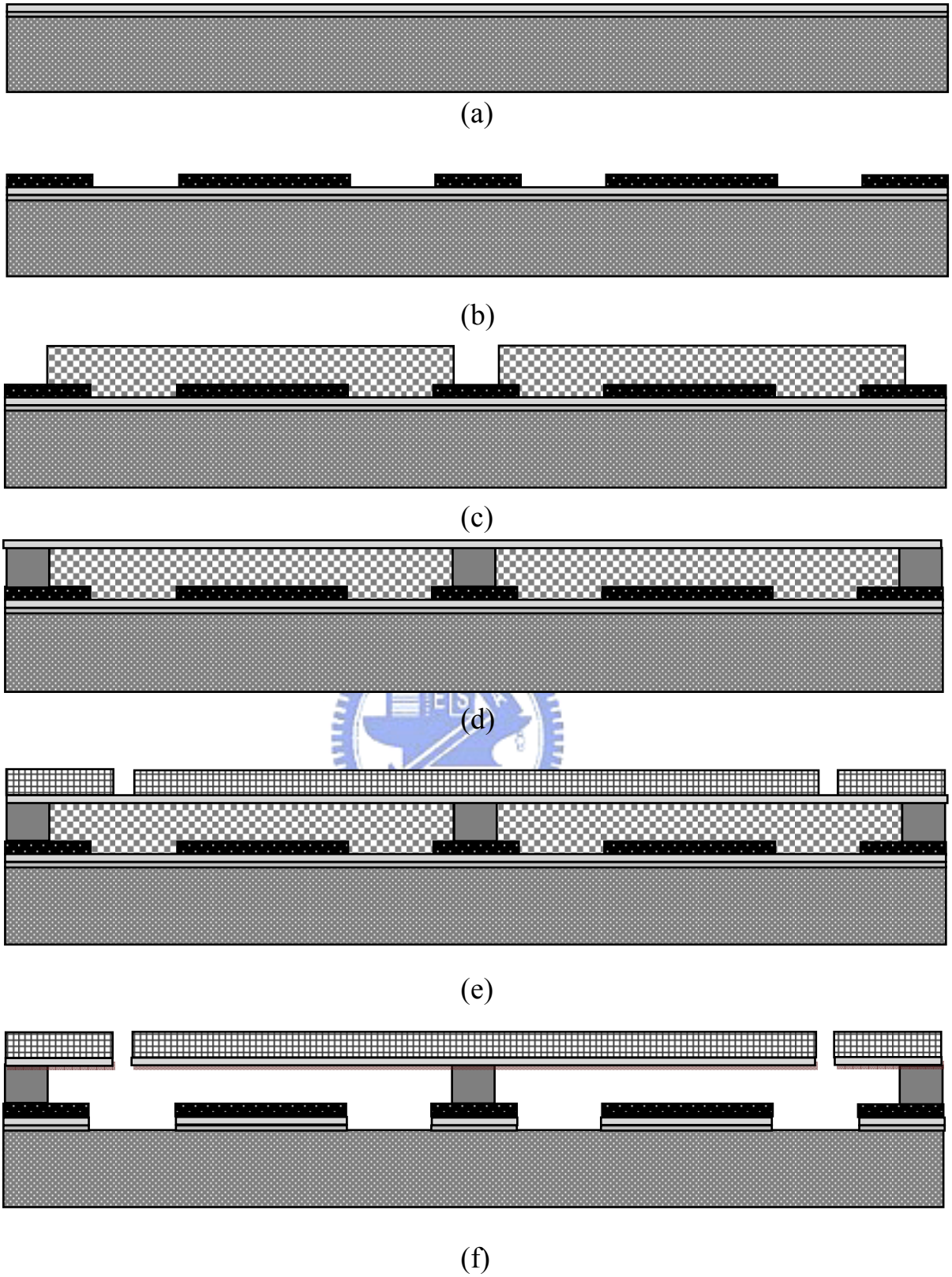

Fig. 3-1 Process sequence for the biomimetic diaphragm of the microphone

Chapter 4 Result and Measurement

4.1 Result of SEM Graph

The fabricated microphone is photographed by Scanning Electro Microscope (SEM) in Fig. 4-1. In Fig. 4-1(a), you can see some holes on all diaphragms. The purpose of these holes whose diameters are 10μm is in order to release the structure more easily. Bottom electrodes and a central-supporting pillar connect copper lines to the contacts for measurement demand. In Fig. 4-1(b), the enlarge view in details of serpentine spring and central gimbals region are displayed. According to this image, using the multimeter to demonstrate that the upper and bottom electrode is not a short circuit; we can say that the structure is successful in the process.

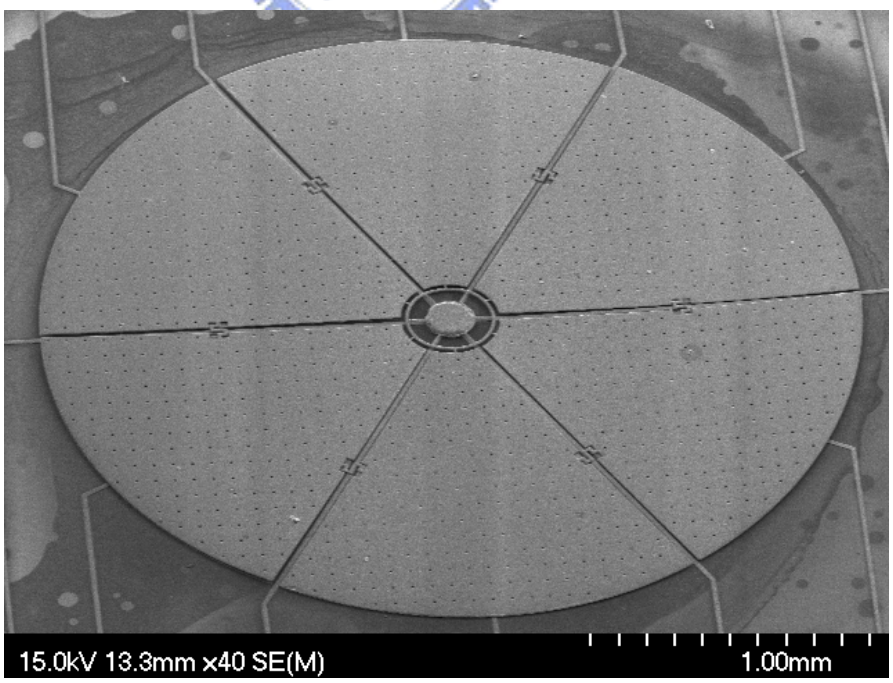

Fig. 4-1(a) The entire view of the microphone is photographed by SEM

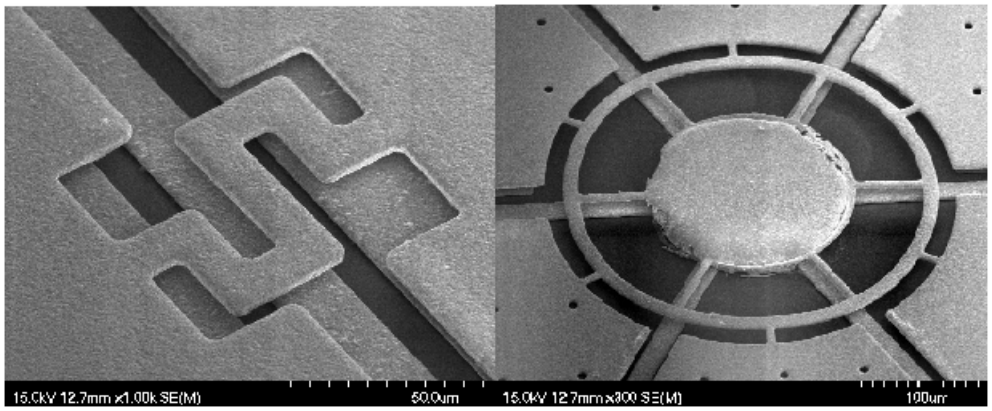

Fig. 4-1(b) The enlarge view photographs focus on the serpentine spring and central gimbals region respectively

4.2 Measurement

In order to confirm the performance of the microphone structure such as the sound-localization and the resonant frequency, we set up the experiment to test the vibration of the microphone around 360 degrees. Fig. 4-2 is the schematic experiment setup for measuring the microphone. The MEMS Motion Analyzer (MMA) owned by National Chip Implementation Center in Taiwan can measure the characteristic of the dynamic displacement of the object which must be periodic motion. In the measurement of the resonant frequency of the diaphragm, the device placed on the platform connected to the High Voltage Amplifier (HVA) which is a piezoelectric actuator. The HVA can provide the device an input periodic signal (sine wave) force on different frequency. The interferometer of the MMA detects the maximum displacement on the specific frequency to get the resonant frequency. The result shown in Fig. 4-3 is about 125±4%Hz which is higher than the simulation by ANSYS.

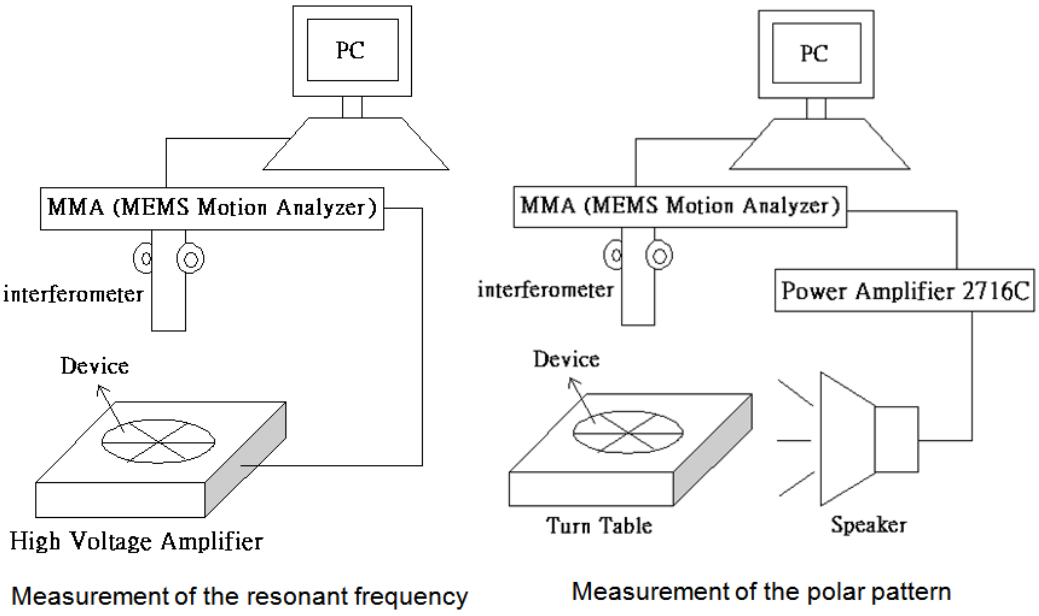

Fig. 4-2 A experiment setup for measuring the microphone

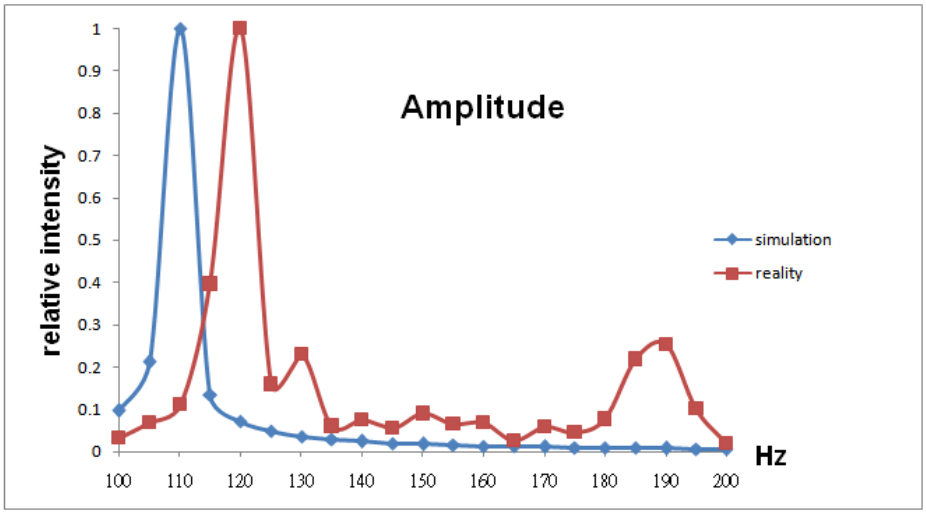

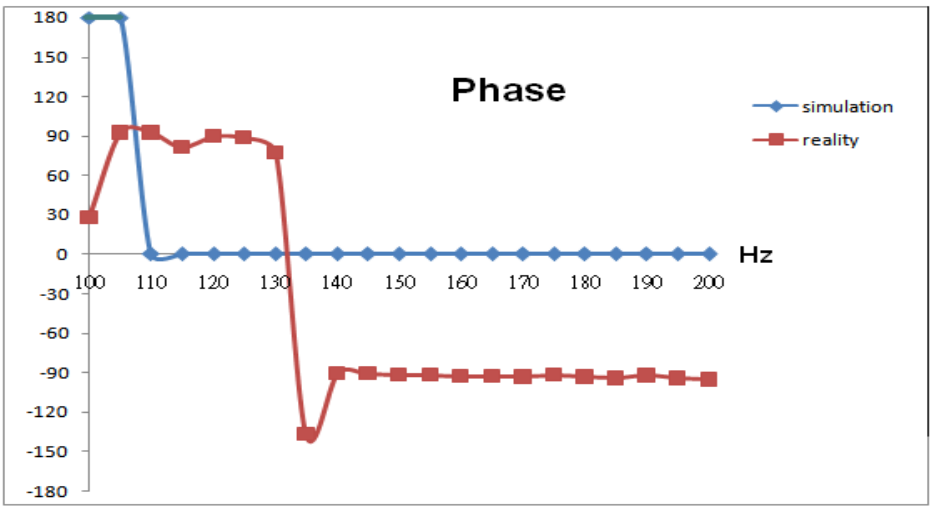

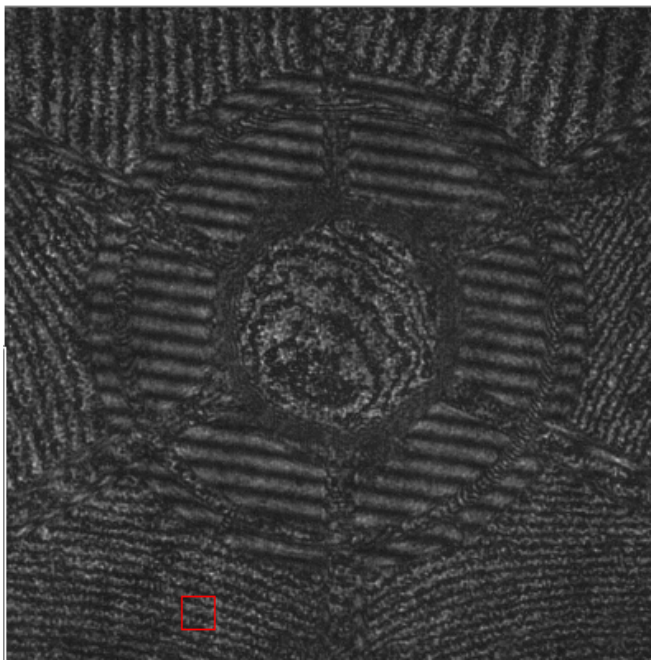

Fig. 4-3 The resonant frequency of the diaphragm measured by MMA and simulation

In the measurement of the polar pattern of the diaphragm, the speaker through the power amplifier connects to the MMA. The device is placed on the turntable which is convenient to measure data around 360 degrees. We choose 300Hz sinusoid sound wave which has larger displacement than other frequency. The plot of the displacement of the diaphragm to the amplitude of the sound source shown in Fig. 4-4 presents that the experiment setup is working but the trend line measured is smaller than simulation. However, the maximum net displacement is only 0.02091μm in 60dB SPL which is measured by B&K microphone 4190L1 calibrated on 94dB, 1 kHz, and this is smaller than simulation value 1.975μm. The polar pattern is shown in Fig. 4-5. The polar pattern in reality has six open angles in 0°~30°, 50°~80°, 110°~130°, 190°~210°, 250°~270° and 290°~320° whose range 25°±20% is bigger than

simulation. However, the shape in reality is like the simulation which has six shaped leaves.

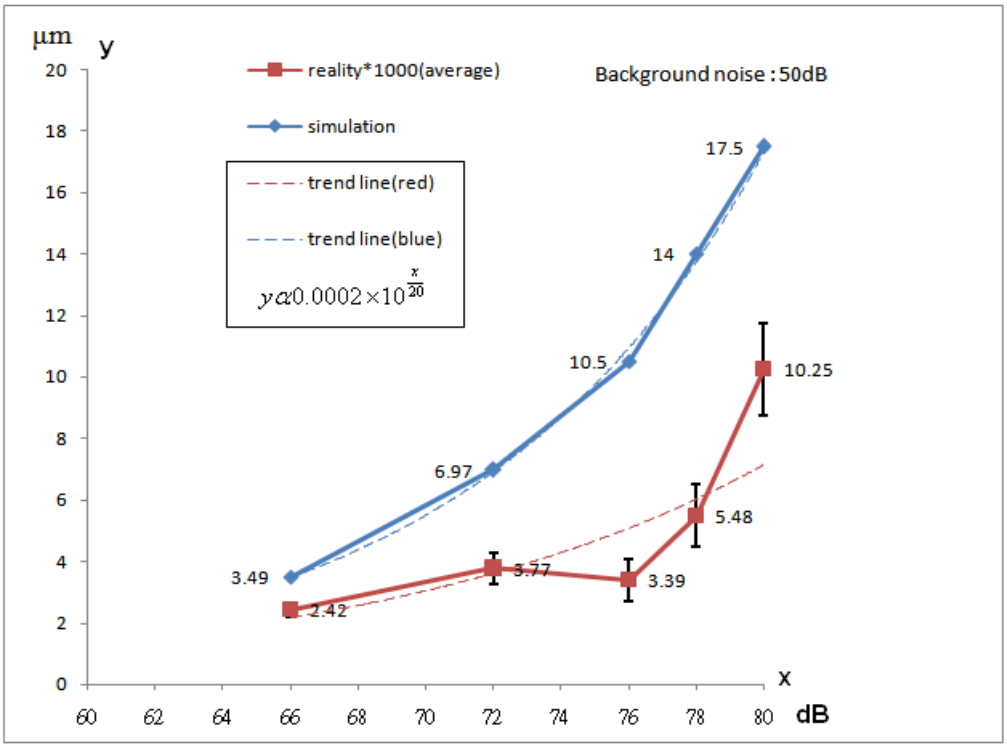

Fig. 4-4 The plot of the displacement of the diaphragm to the amplitude of the sound source between reality and simulation

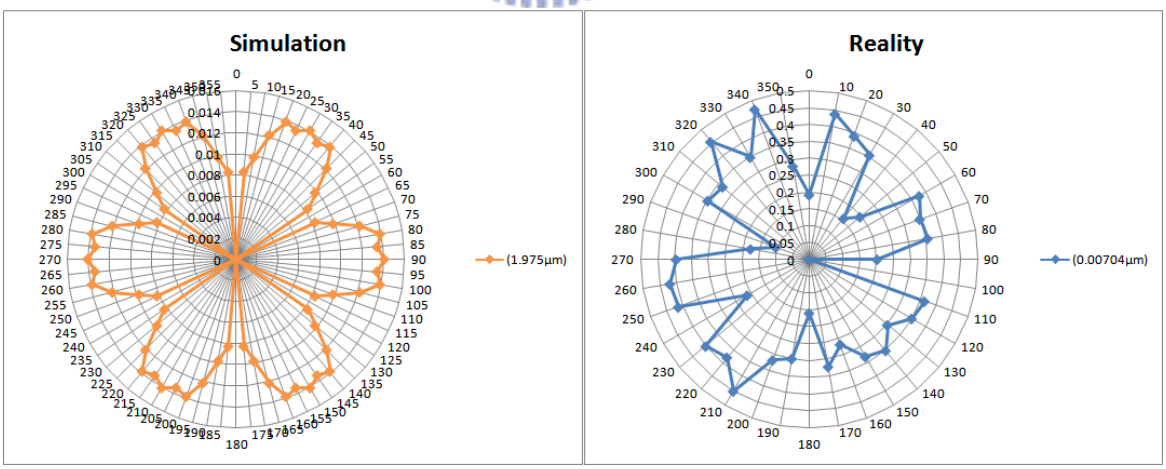

Fig. 4-5 The polar pattern of upward displacement of the diaphragm in 60dB SPL, 300Hz (reference displacement in simulation: 1.975μm; in reality: 0.00704μm)

4.3 Discussion

We will discuss the unexpected result and some issues below. The surface roughness of the central gimbals region and any diaphragm region obtained by WYKO analysis system is shown in Fig. 4-6(a)(b). The non-smooth surface with the deformation around the diaphragm after the release step of the fabrication may be resulted from the stress between copper and liquor. Another reason for the deformation is that the simple electroplating copper installation causes a not good quality of the copper diaphragm.

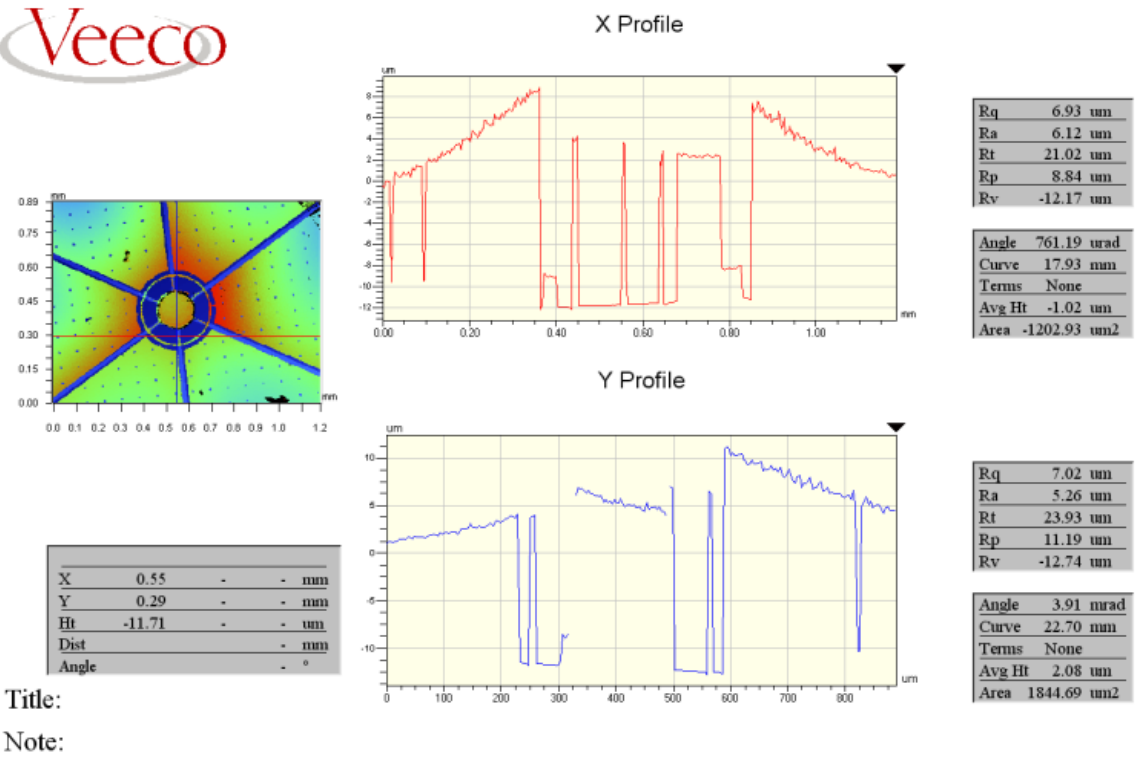

Fig. 4-6(a) The surface roughness of the central gimbals region obtained by WYKO analysis system

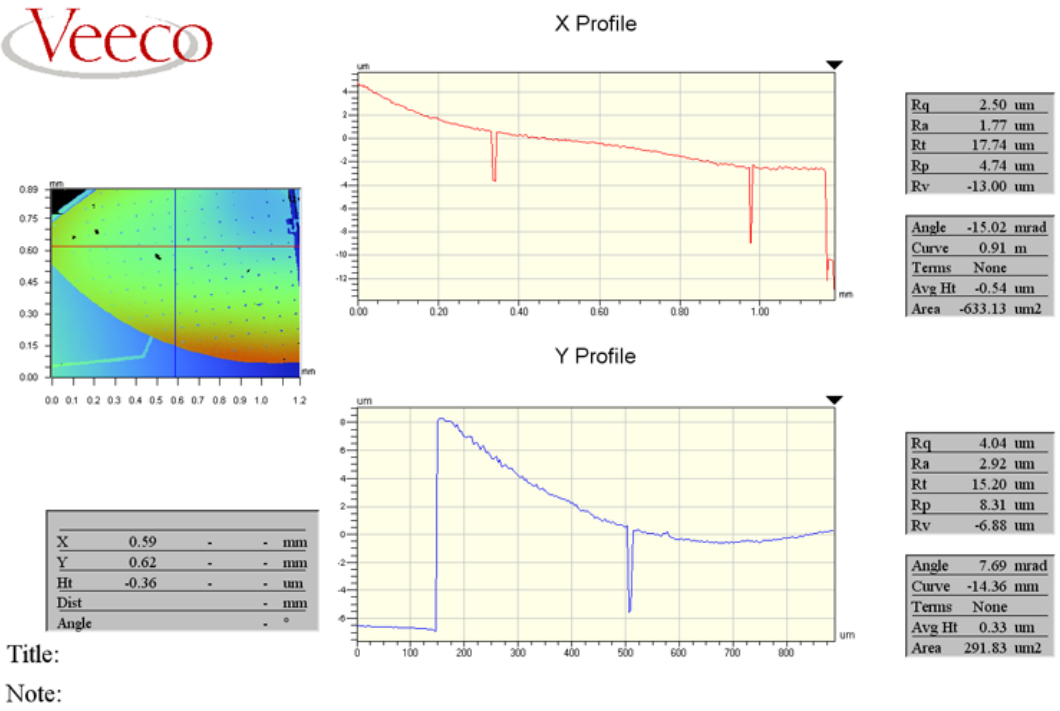

Fig. 4-6(b) The surface roughness of one diaphragm region obtained by WYKO analysis system

In order to demonstrate the influence of the deformation, we use ANSYS to simulate the correction structure which has 8μm of tilt on the end of the diaphragm shown in Fig. 4-7. The result is shown in Fig. 4-8. The simulation can explain that the deformation of the diaphragm results in the decrease of the performance. That is why we measure the small displacement of the real diaphragm. Table 2 shows the correction properties is similar to the properties in reality.

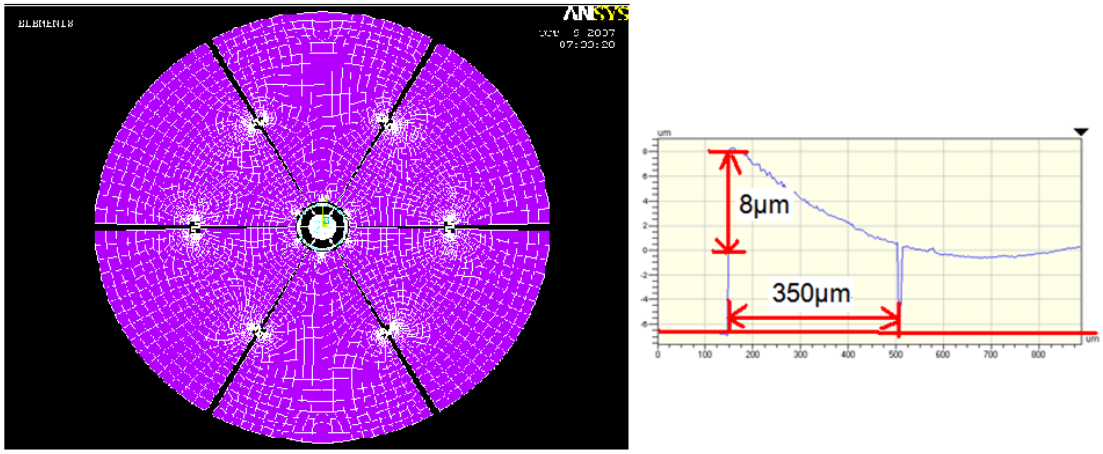

Fig. 4-7 The correction structure by ANSYS simulation

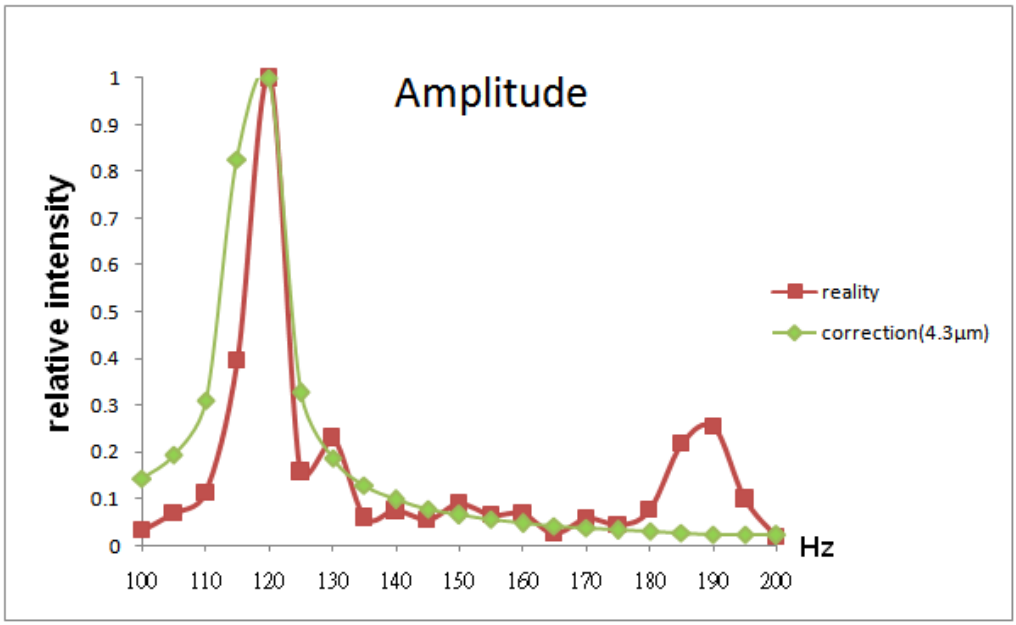

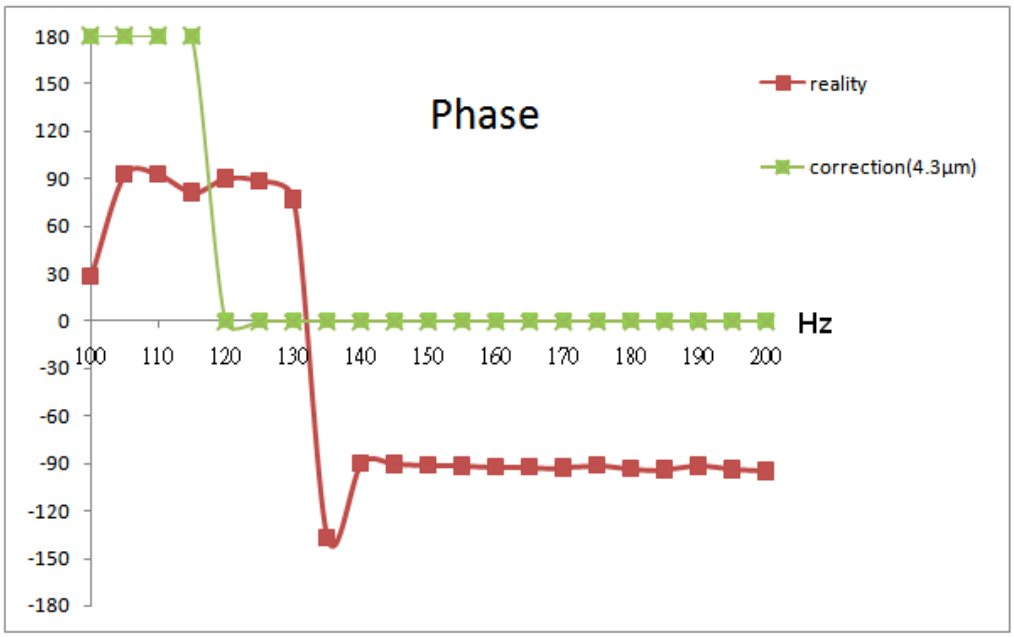

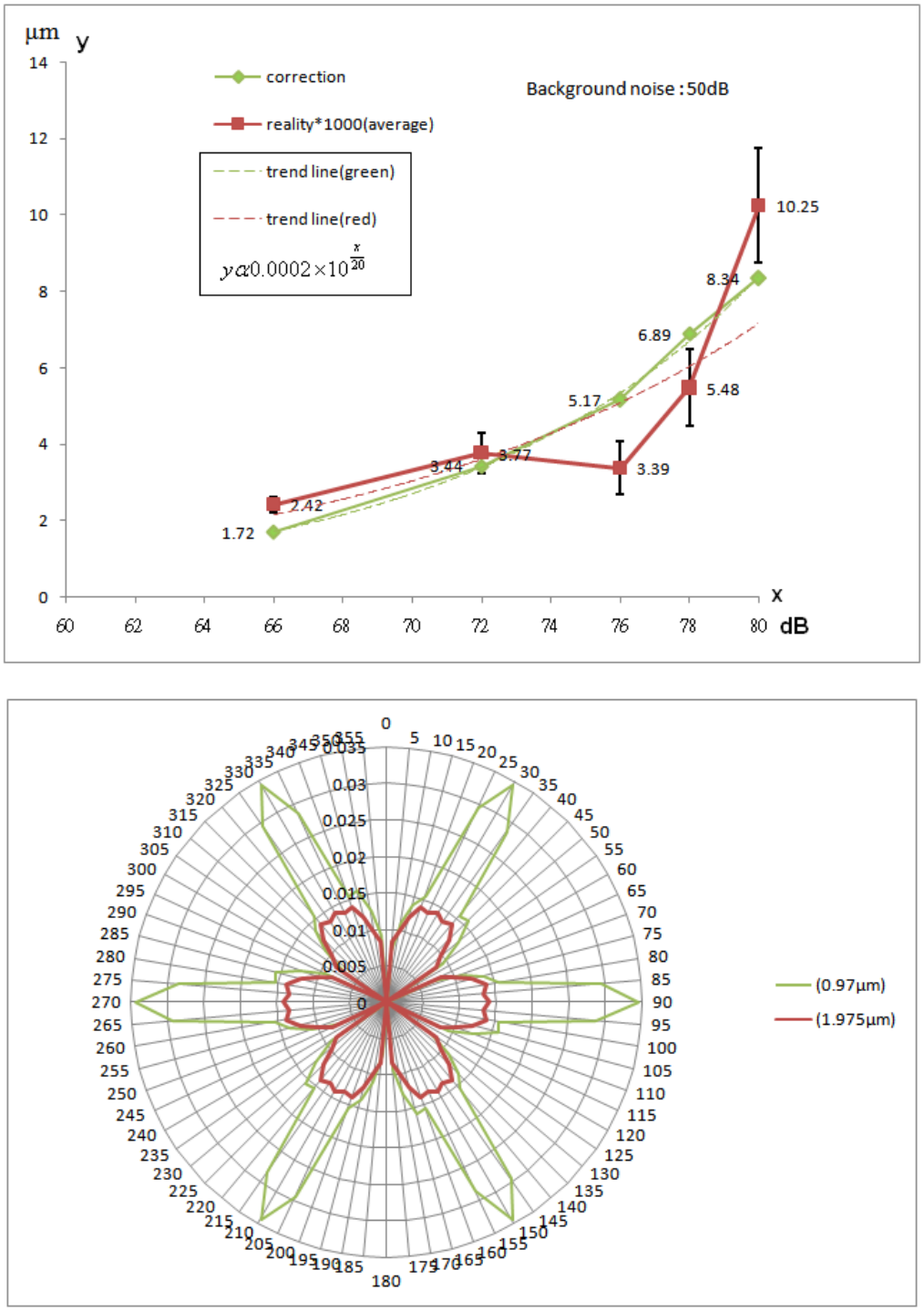

Fig. 4-8 The ANSYS simulation of the deformation of the diaphragm

Comparison between reality and simulation	60dB Maximum net displacement	in-phase resonant mode
Reality	0.02091μm	125±4%Hz
Simulation(4μm)	2.04μm	110Hz
Correction(4.3μm)	1.05μm	120Hz

Table 4-1 Comparisons of the microphone properties between reality and simulation.

Chapter 5 Conclusion and Future Work

5.1 Conclusion

Even though the performance of the microphone fabricated by copper is not ideal, the structure is successful in the process. Improvement in fabrication process and experiment setup is required, for example, electroplating copper using professional equipment and measuring the variation of the capacitor between upper electrode and bottom electrode. However, the resonant frequency is so low that the user is not comfortable and we will improve the structure size to raise the resonant frequency.

$$F = k_{beam} \times x = P_{constant} \times A_{leaf} \qquad k_{beam} \alpha E t_{leaf}^{\ 3}$$

$$f_{resonant} = \frac{1}{2\pi}\sqrt{\frac{k_{beam}}{m_{leaf}}} = \frac{1}{2\pi}\sqrt{\frac{k_{beam}}{A_{leaf} \times t_{leaf} \times \rho_{leaf}}}$$

By above equations [12], decrease of the density of the material(ρ_{leaf}) can raise the resonant frequency but not reduce the displacement.

5.2 Future Work

In the future, we will find the suitable material and overcome the difficult in fabricated process to make a better MEMS directional microphone.

References

[1]Akihito Saito, Nobutaka Ono, and Shigeru Ando, “Micro Gimbal Diaphragm for Sound Source Localization with Mimicking Ormia Ochracea,” *SICE*, Vol. 4, pp. 2159-2162, Aug. 2002

[2]Nobutaka Ono, Akihito Saito, and Shigeru Ando, “Design and Experiments of Bio-mimicry Sound Source Localization Sensor with Gimbal-Supported Circular Diaphragm,” *Solid-State Sensors and Actuators, Transducers’03*, pp. 939-942, Jun. 2003.

[3]Nobutaka Ono, Akihito Saito, and Shigeru Ando, “Bio-mimicry Sound Source Localization with Gimbal Diaphragm,” *T.IEE Japan*, Vol. 123-E, No. 3, pp. 92-97, Mar. 2003.

[4]N. Ono, T. Arita, Y. Senjo, and S. Ando, “Directivity Steering Principle for Biomimicry Silicon Microphone,” *Solid-State Sensors and Actuators, Transducers’05*, pp. 792-795, Jun. 2005.

[5]Daniel Robert, John Armoroso, and Ronald R. Hoy, “The Evolutionary Convergence of Hearing in a Parasitoid Fly and Its Cricket Host,” *Science*, Vol. 258, pp. 1135-1137, Nov. 1992.

[6]R. N. Miles, D. Robert, and R. R. Hoy, “Mechanically coupled ears for directional hearing in the parasitoid fly Ormia ochracea,” J. Acoust. Soc. Am, Vol. 98, No. 6, pp. 3059-3070, Dec. 1995.

[7]Wen Hao Ching and Y. T. Cheng, “Design and Fabrication of High Performance Sound-Localized Microphone Using Oxalis-like Sensing Diaphragm,” National Chiao Tung University, Taiwan, 2006.

[8]P. C. Hsu, C. H. Mastranglo, “A high sensitivity polysilicon diaphragm condenser microphone,” IEEE, 1998.

[9]Tinghui Xin, Pratul K. Ajmera*, Chuang Zhang, and Ashok Srivastava, “Post-CMOS chip-level processing for high-aspect-ratio microprobe fabrication utilizing pulse plating,” proceeding of SPIE, Vol 5763, pp.1-10, 2005.

[10]X. Li, R. Lin, H. Kek, J. Miao, and Q. Zou, “Sensitivity-improved silicon condenser microphone with a novel single deeply corrugated diaphragm,” Sensors and Actuators A 92, pp.257-262, 2001.

[11]ANSYS, http://www.ansys.com/ 9.0 version.

[12]Roy R. Craig, Jr. Mechanics of Materials, 2nd New York: Wiley, 1999

Vita

姓　　名：劉濬誠 (Chun-Cheng Liu)

出生日期：1983 年 7 月 14 日

出 生 地：高雄市

E - mail：jyunchen.ee94g@nctu.edu.tw

學　　歷：

高雄市立高雄高級中學　　(1998.9～2001.6)
(Kaohsiung Municipal Kaohsiung Senior High School)

國立交通大學電機與控制工程學系　　(2001.9～2005.6)
(Department of Electrical and Control Engineering, Nation Chiao-Tung University)

國立交通大學電子工程所碩士班　　(2005.9～2007.10)
(Institute of Electronics, Nation Chiao-Tung University)